Adsorption and Isotherm Studies of Disperse Orange 44 Dye Using Iron Oxide Nanoparticles

Mohamed M. Hammam[(a)], Youssef Abdo [(b)], Hoda A. Elsawy[(b)*]

[a]Department of Basic Sciences, Faculty of Energy and Environmental Engineering, The British University in Egypt El-Sherouk City, Egypt
[b]Department of Chemical Engineering, Faculty of Engineering, The British University in Egypt El-Sherouk City, Egypt

DOI: https://doi.org/10.56293/IJASR.2024.6108

IJASR 2024
VOLUME 7
ISSUE 5 SEPTEMBER - OCTOBER **ISSN: 2581-7876**

Abstract: An overwhelming source of polluted water originates from chemical companies, with the textile industry being the most hazardous as it uses the most non-biodegradable organic dying compounds. These dyes are designed to resist decomposition, last for a very long time, and, if not removed, could harm the environment. This Research uses the adsorption technique to remove organic disperse orange 44 dye from water using hematite nanoparticles. Hematite used in the adsorption process is straightforward, affordable, and environmentally acceptable, this was accomplished through the precipitation method between iron nitrate salt and NaOH. Moreover, XRD, SEM, and FT-IR will be used to fully characterize the Hematite surface, the optimal parameters with the greatest color removal, was found to be at contact time of 150 min, pH value of 2, concentration of dye of 7 ppm, and adsorbent dosage of 0.15 grams, resulted in a removal of 85.57%. Moreover, Isotherm study was conducted on the adsorption process, and it's observed that adsorption best fit the Langmuir isothermal model more than Freundlich, Halsey, BET, and Dubinin-Radushkevich models.

Keywords: Orange 44 Dye, Adsorption, XRD, SEM, FT-IR, Hematite, Isotherm

Introduction

Natural and synthetic dyes fall into two major categories. Natural dyes are those that are produced from plants, bugs, or minerals. Vegetable dyes, which are typically sourced from plant materials including roots, berries, wood, plants, and wood in addition to biological sources like fungi, make up most natural colors. (Kassinger, 2003). A lot of techniques can be used for the removal of dyes from wastewater like electrocoagulation, filtrations, activated sludge, squinching batch reactors, ion − exchange resins, coagulation, flocculation, and adsorption. (Ghosh & Webster, 2022). Adsorption is regarded as a quick, inexpensive, straightforward, sludge-free process with great selectivity and efficiency. (Badr M.Thamer, 2019). It is well known that adsorbent materials have advantageous surface physics-chemical properties that allow them to bind to various contaminants in aqueous media. The complexity of wastewater generation caused by the variety of contaminants present calls for excellent efficiency from absorbents. A more modern adsorbent needs to be more selective, perform better in terms of adsorbent dosage over a wider pH & pollutant concentration range, and have faster kinetics. The cost effectiveness of creating the adsorbent material depends on the economy of the treatment process, but so does its ability to regenerate. The physical and chemical features of Iron nano particles, which can be produced from synthetic or biological waste sources have allowed for faster and more effective binding to various contaminants. (Krstić, 2021). In this research we aim to synthesize and characterize Iron oxide nanoparticles and use it to remove disperse orange 44 dye from water then studying the best conditions for the dye removal and the reaction isotherm.

Materials and Methods

Materials

Iron oxide nano particles were synthesized by using Iron (III) Nitrate salt Fe $(NO_3)_3$, Isobutanol ($C_4H_{10}O$), Ethanol (C_2H_5OH), sodium hydroxide (NaOH), and double Distilled Water. An industrial wastewater was simulated using Disperse orange 44 ($C_{18}H_{15}ClN_6O_2$) as a representative textile dye.

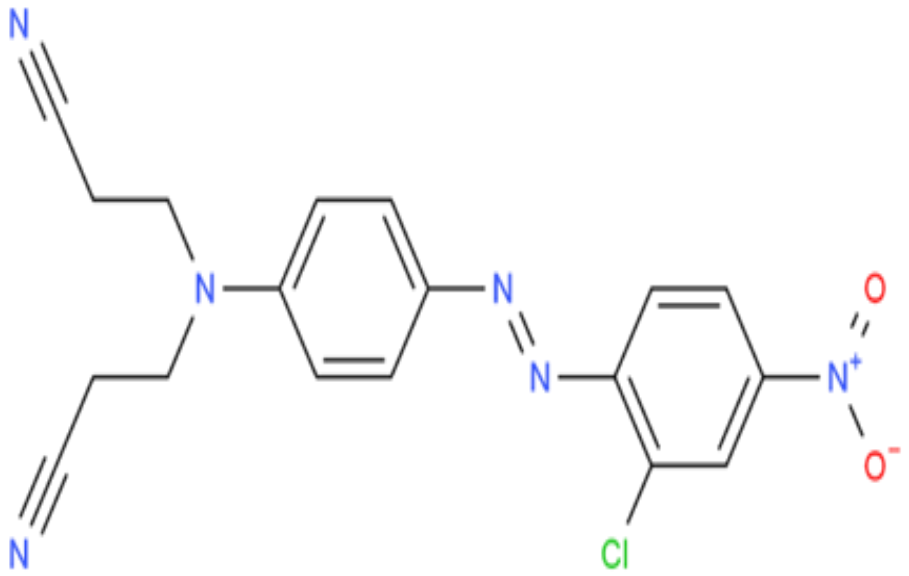

Figure 1: Disperse Orange 44 chemical structure.

Methodology

Hematite Crystals or (Iron oxide nano particles) were synthesized by precipitation. For this purpose, Iron (III) nitrate salts (2 g) were dissolved in iso-butanol alcohol (50 mL), where the mixture was stirred for two hours at $75^{o}C$, then 0.1M NaOH was added dropwise for the whole iron oxide nano particles generation time (two hours). The solution was dried and calcined for two hours at a temperature of $400^{o}C$, then for five consequent hours at a temperature of $600^{o}C$. Synthesized iron oxide nano particles are then collected and crashed genuinely using a specific crashing tool. (Jabbar, 2022)

A stock solution of disperse orange (100 mg/L) was prepared in distilled water, where the desired concentrations were obtained by dilution from the stock solution.

Instruments

Cary 5000 UV-Vis-NIR Device that was manufactured by Agilent company in Malaysia for measurements of FTIR. Panalytical empyrean (3) device from Malvern company, Netherlands for XRD measurements. Thermofisher (USA) Quattro S field emission gun equipped with EDX machine for SEM determination.

Results and Discussion

Characterization of Iron Oxide Nanoparticles

FTIR Analysis

FT-IR for hematite before it has been used in the removal process, the sharp peaks at the 440.96, and 518.82 cm^{-1} indicated the formation of the iron oxide nano particles (hematite), which comes in good agreement with values previously researchers. (Noruozi & Nezamzadeh-Ejhieh, 2020). A peak at a value of 1018.53 cm^{-1} was observed which may represent the stretching vibrations of the $(Fe - O)$ bond in the hematite. The peaks in the fingerprint region are intact, which indicates that no chemical changes have occurred to hematite. However, the stretching vibrations of the $(Fe - O)$ bond in the hematite has shifted from 1018.53 to 1034.1 cm^{-1}, additionally its intensity has significantly decreased, which indicates the adsorption of the dye.

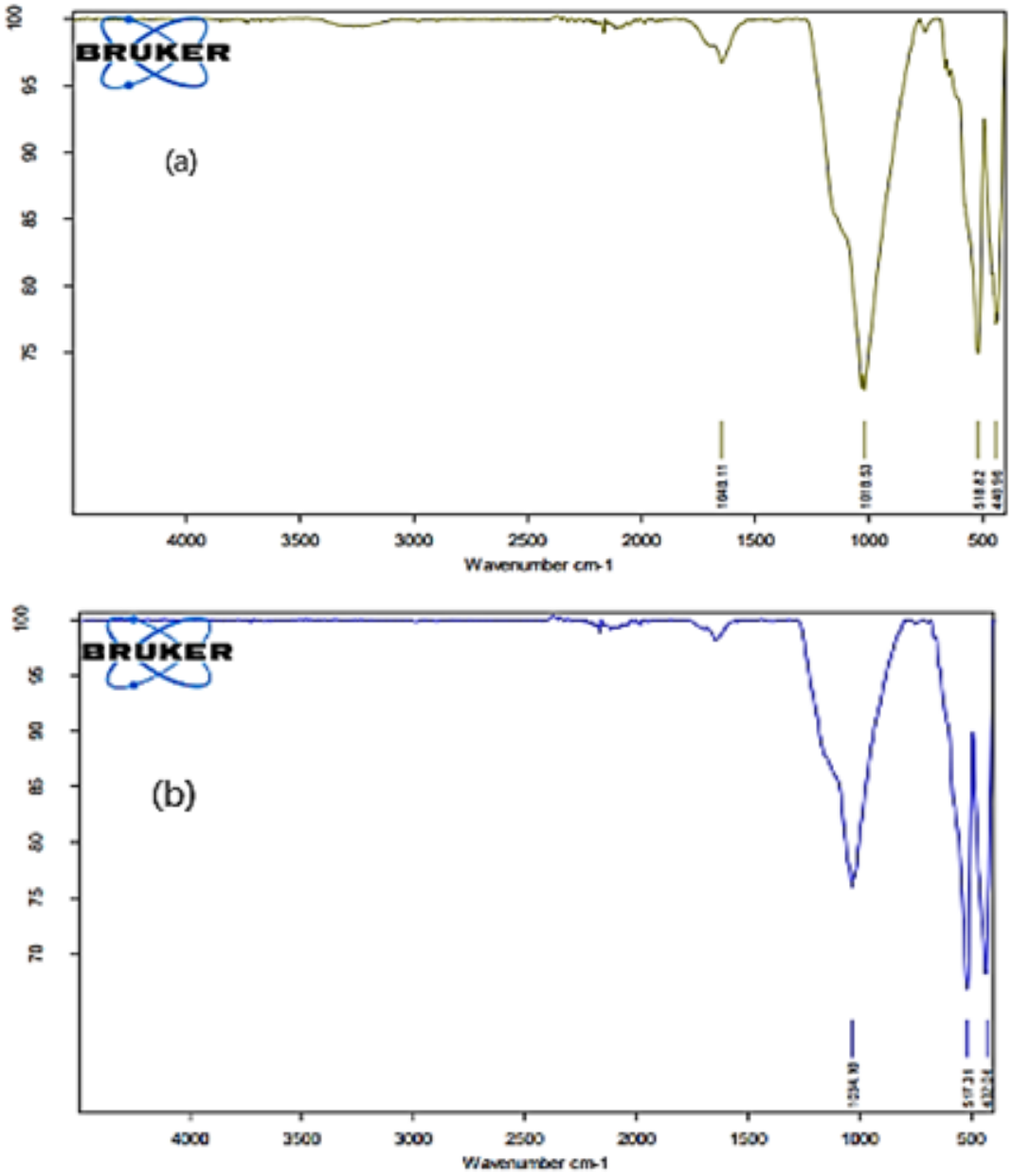

Figure 2. Hematite FT-IR Spectrum analysis (a) Before the Adsorption of the dye and (b) after the adsorption of the dye

XRD Analysis

The synthesized hematite has a = b = 5.0342 Å, c = 13.7321 Å, the hematite lattice structure is rhombohedral with a space group of R-3C, the alpha = beta = 90.0°, and the gamma = 120.0°. (Ullmann, 2000). Comparing the synthesized hematite nano particles with the JCDPS (Joint committee on powder diffraction standard) card number 33-0664, an XRD diffraction peaks, and diffraction planes of 24.1° (0 1 2), 29.5° (1 1 0), 33.1° (1 0 4), 35.6° (1 1 0), 36.4° (1 1 1), 42.2° (2 0 0), 49.5°(0 2 4), 54.0° (1 1 6), 61.0° (2 2 0), 62.4° (2 1 4), 63.9° (3 0 0), and 73.5° (3 1 1) were observed which came in perfect agreement with synthesized hematite indicating the success of the synthesis procedure as shown in Figure 3.

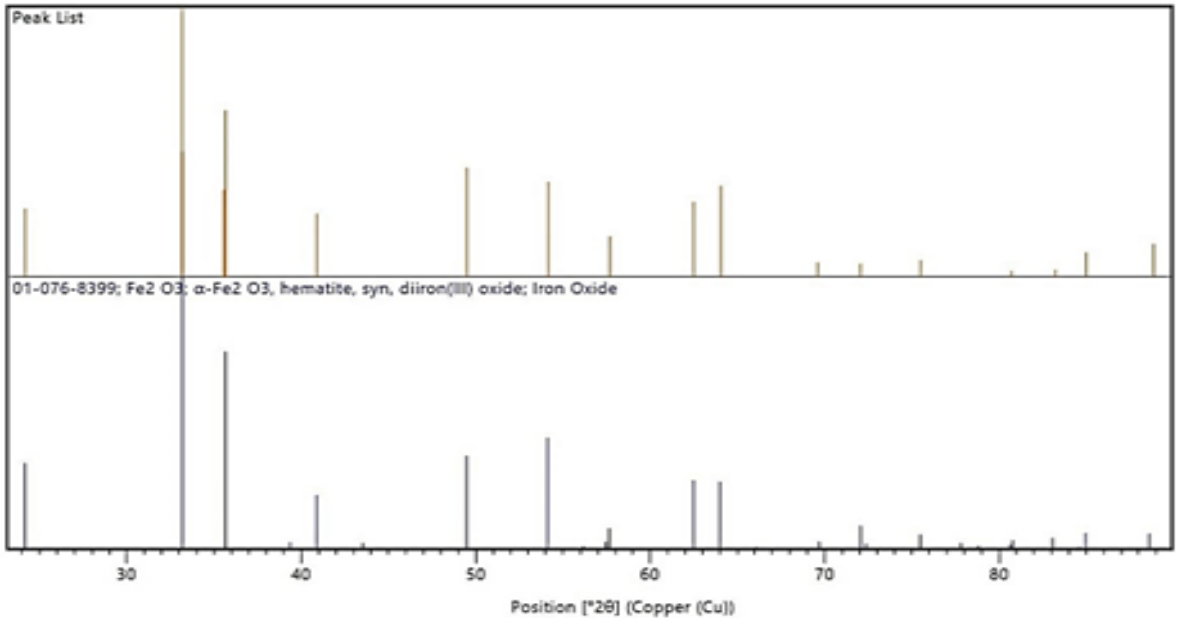

Figure 3. Comparing the Diffraction peaks of the synthesised hematite with another hematite card (the yellow one).

After the adsorption process, the $\alpha - Fe_2O_3$ shows a significant decrease in the hematite peak intensity and also the diffraction peaks at 2θ have shifted significantly. New peaks have appeared in the spectrum, indicating the formation of new phases. Alternatively, some peaks have disappeared which indicates a change in the crystal structure or that some components have been removed as shown in Figure 4.

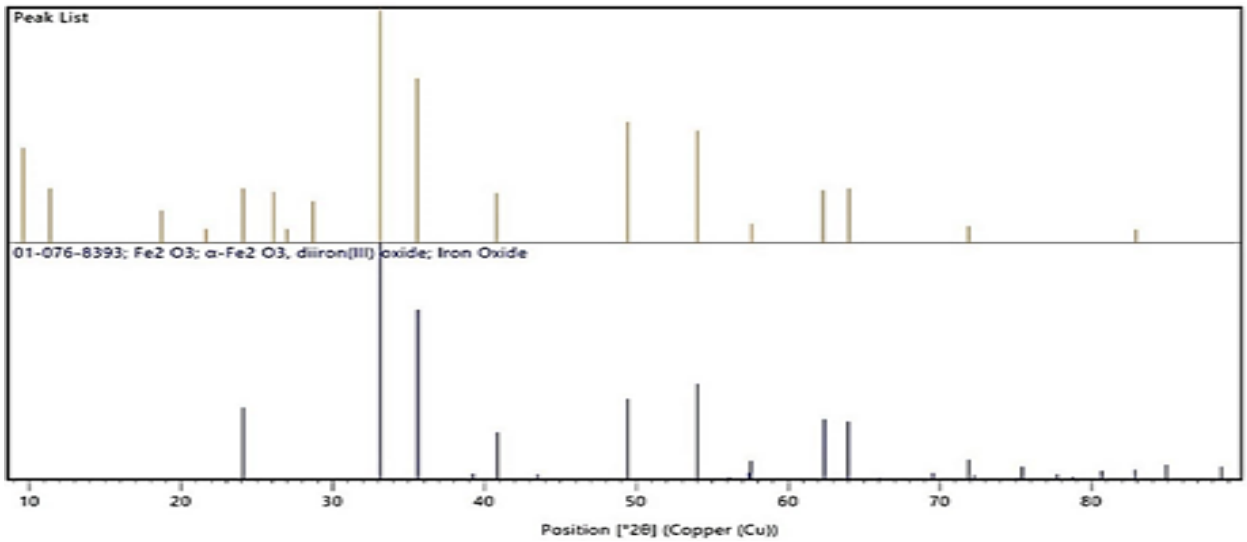

Figure 4. Comparison between Sample after adsorption (yellow peaks) and the original sample.

SEM Analysis

The SEM image (Figure 5) shows a clear distribution of the hematite particle in normal morphology, also some aggregate may have been formed, the SEM also helps illustrate whether the particles are monodispersed or a polydisperse which is shown as a polydisperse. The hematite particles have a spherical morphology or a disk-like morphology, the agglomeration of the hematite nano particles is due to the van der Waals forces between the hematite particles.

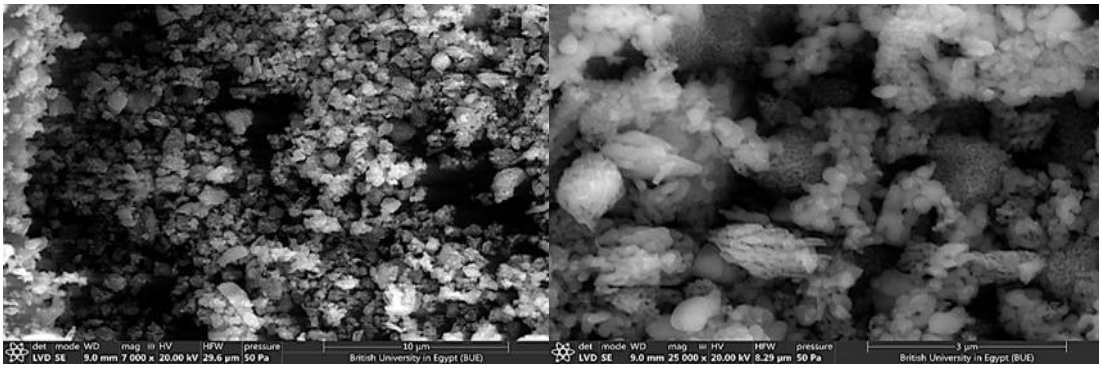

Figure 5. SEM photograph of the Hematite Nano Particles

The particles after the adsorption process seem to have larger particle size and more strong agglomerations through chemical bond and van der Waals forces, the material surface structure also seems to be lees rough than the original sample which indicate the formation of amorphous phase (Figure 6), which is further evidence that indicates the adsorption of the dye on the surface of hematite which comes in line with the previous tests.

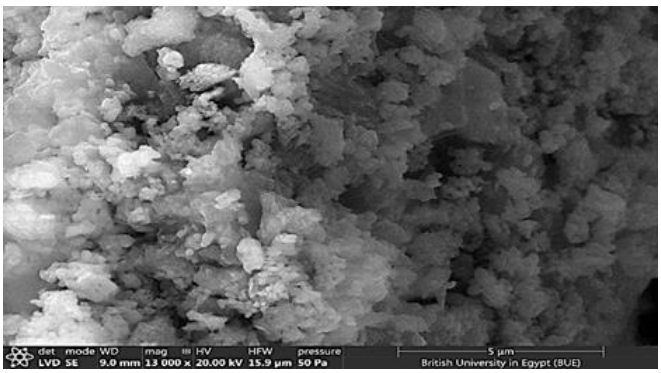

Figure 6. SEM photograph of the Hematite Nano Particles after the adsorption process

Disperse Orange 44 Dye Characterization

Wavelength scan for the dye was conducted and the maximum light absorbance of the organic disperse orange 44 dye was found to be at maximum wavelength of $\lambda max = 585\ nm$. Consequently, a calibration curve was plotted between the different concentrations of the dye and their corresponding absorbance, to later determine the concentration of the dye at equilibrium after carrying out the adsorption process.

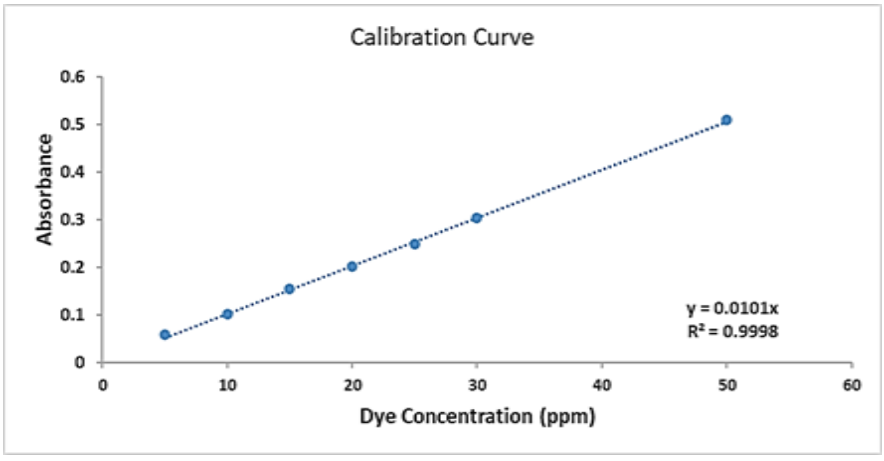

Figure 7. Calibration Curve of Disperse Orange 44 Dye

Studying the optimum conditions for the adsorption of the dye

Optimum contact time

The graph shows that the removal of the organic dye from the water sample is increasing by increasing the contact time between the adsorbent and the adsorbate and observed to be 150 minutes resulted in a dye removal % = 78.7 % of the initial 45 (ppm) dye concentration.

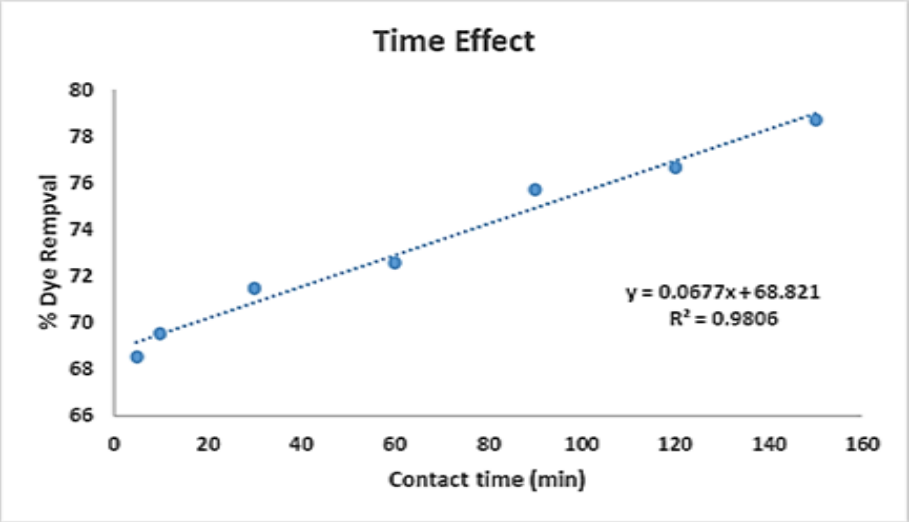

Figure 8. corresponding dye removal% to its Contact time graphical representation

Optimum pH value

The Adsorption of the dye by the hematite adsorbent nanoparticles was best at very high acidic medium (lower pH) in the water solution sample of pH value = 2. As shown in the following graphical chart.

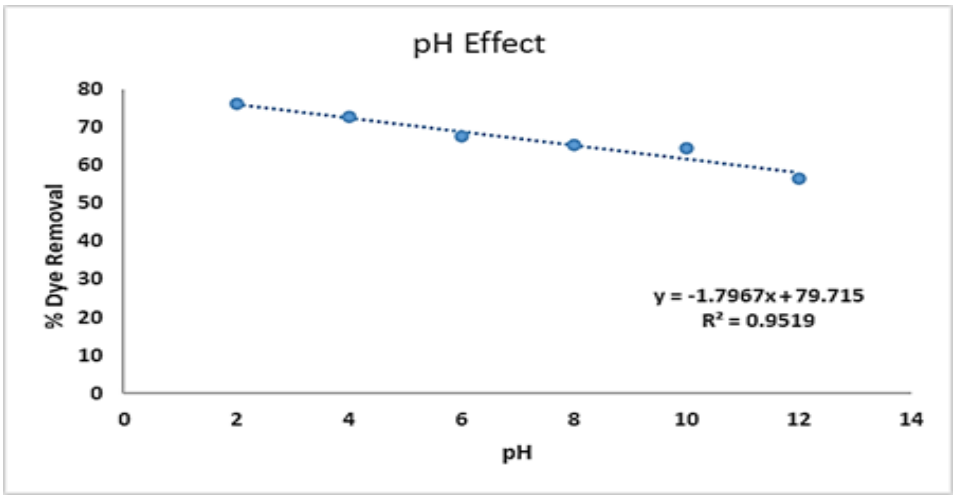

Figure 9. corresponding dye removal% to pH change

Optimum Dye concentration

Figer 10 shows an inverse relationship between increasing the initial dye concentration and the removal% of the organic disperse orange 44 dye. The optimum removal was found at a dye concentration of 7 (ppm) where ≈ 85% of the dye was removed.

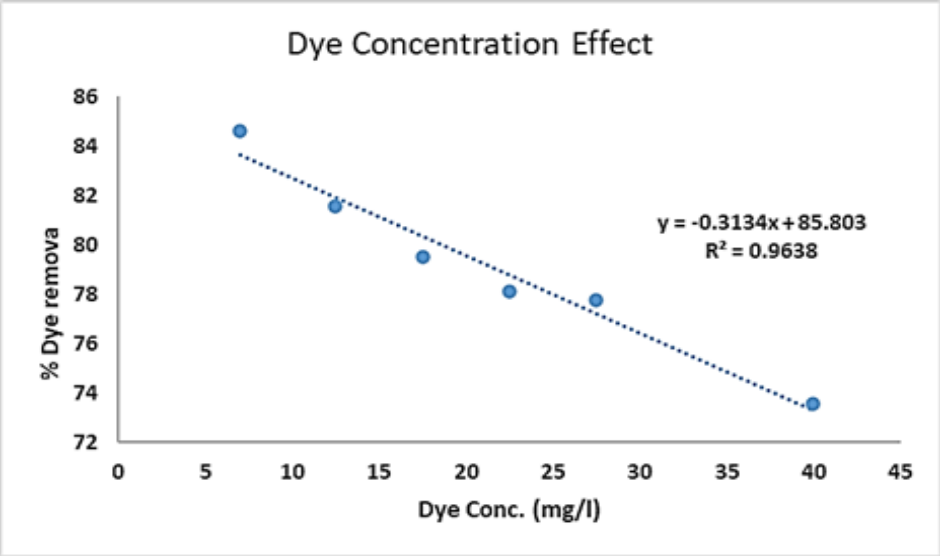

Figure 10. corresponding dye removal% to the change of the initial dye concentration

Optimum Hematite Nanoparticles dose

The optimum hematite adsorbent dosage was found to be at the highest dose used of 0.15 grams.

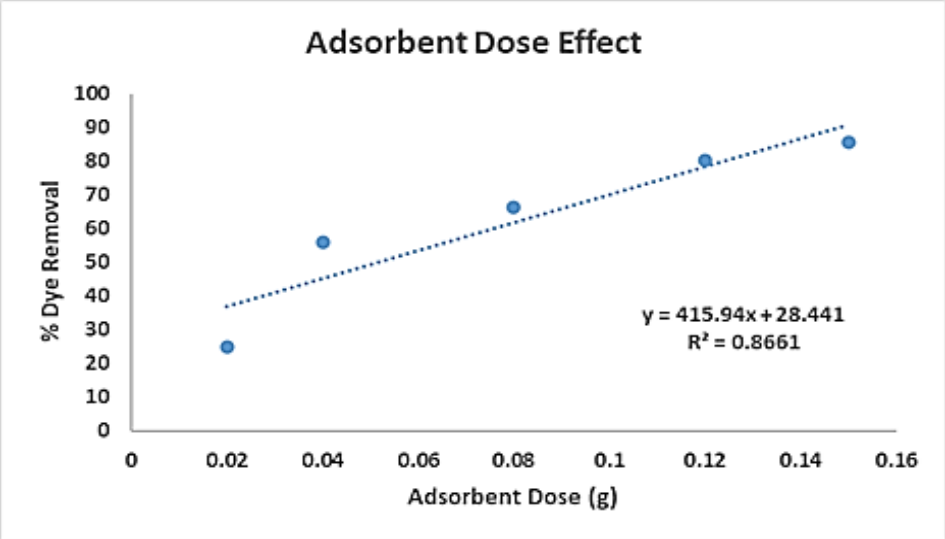

Figure 11. corresponding dye removal% to the change of the Hematite adsorbent dose

Isotherm Study

Various isotherm models were tried for studying the adsorption mechanism. The results observed indicate that the R^2 Values of both Halsey and Freundlich isotherm are the best models to represent the adsorption process as they have the highest R^2 Values = 0.9983, however because the Freundlich isotherm model has a negative intercept, and the Halsey isotherm has a negative slope value, they cannot be used as the best models to describe the adsorption process.

On the other hand, the Langmuir isotherm turns a relatively smaller R^2 Value of 0.9589, which initially may indicate that this model does not have the best data fit to its line, however it has positive intercept and slope values which imply that Langmuir is the best isotherm model, which indicates a monolayer adsorption process on the hematite

surface. Moreover, the Langmuir isotherm further indicates a homogenous surface where all adsorption sites have similar characteristics, and each adsorption site can adsorb one molecule of the dye.

Table 1. Different Isothermal Models Comparison & Results

Isotherm models	Parameters	Values
Langmuir	R^2	0.9589
	q_m (mg/g)	11.4416
	K_L (l/mg)	0.0959
	R_L	0.2066
Freundlich	R^2	0.9983
	n	0.7135
	K_F (l/mg)	0.8468
Halsey	R^2	0.9983
	n_H	0.7135
	K_H (l/mg)	1.1259
BET	R^2	0.8818
	b	0.7640
	q_m (mg/g)	4.7806
Dubinin - Raduskevich	R^2	0.8149
	□	0.5203
	E (KJ/mol K)	0.9803
	q_m (mg/g)	4.1774

Additionally, the Langmuir isotherm can highlight some adsorption behavior according to each parameter in the Langmuir formula, for example, The Q_{max} shows the maximum dye amount that can be adsorbed per unit mass of the hematite, it can identify the saturation point where all the adsorption sites on the hematite surface are filled with dye molecules.

Finally, The Langmuir constant (K) indicates the strength of adsorption between the hematite and the dye. When this constant is higher it means a stronger adsorption, however it does not describe the speed or the rate of adsorption.

Other isothermal models were also studied in this adsorption process such as BET and Dubinin-Radushkevich which both have a negative slope and a low R^2 Values, Table (1) summarizes all the isothermal models constants.

Conclusions

The hematite nanoparticles were successfully prepared using the precipitation method by dissolving the iron (III) nitrate salt in alcohol, distilled water then a solution of 0.1 M NaOH. The nanoparticles were fully characterized using different analytical techniques such as FTIR, SEM and XRD. Afterwards, the nanoparticles were studied for their adsorption ability of disperse orange 44 dye as a representative of the textile dyes. The optimum conditions for the adsorption process were evaluated at a time of 150 minutes, pH 2, initial dye concentration of 7 ppm and hematite dose of 0.15 gm which resulted in a removal of 85.573% of the dye in the wastewater sample. Several adsorption isotherm studies were conducted to verify the mechanism and nature of the adsorption process. It was found that the adsorption process is best described by Langmuir isothermal model.

References

1. Ali, D. A. (2023). Kinetics and Isotherm Studies for Adsorption of Gentian Violet Dye from Aqueous Solutions Using Synthesized Hydroxyapatite. Journal of Environmental and Public Health. 2023. doi.org/10.1155/2023/741877.
2. Badr M.Thamer, A. A.-H.-E.-N. (2019, Aug). Effective adsorption of Coomassie brilliant blue dye using poly (phenylene diamine) grafted electrospun carbon nanofibers as a novel adsorbent. Materials Chemistry and Physics, 62 230.doi:https://doi.org/10.1016/j.matchemphys.2019.05.087.
3. Kassinger, R. (2003). Dyes: From Sea Snails to Synthetics. Twenty-First Century Books. doi:0761321128.
4. Kirk-Othmer. (2004). Kirk-Othmer Encyclopedia of Chemical Technology, 27 Volume Set. Wiley, 2004. doi:10.1002/0471238961.
5. Krstić, V. (2021). Handbook of Nanomaterials for Wastewater Treatment.doi:https://doi.org/10.1016/B978-0-12-821496-1.00024-6.
6. Singh, A. K. (2016). Structure, Properties and Mechanisms of Toxicity. Engineered Nanoparticles,1-18. doi:https://doi.org/10.1016/B978-0-12-801406-6.00001-7.
7. Ullmann, F. (2000). Ullmann's Encyclopedia of Industrial Chemistry 6th edition. Wiley, 2000. doi:10.1002/14356007.a09_073.Ghosh, S., & Webster, T. J. (2022). Biologically synthesized nanoparticles for dye removal. Development in Wastewater Treatment Research and Processes: Removal of Emerging Contaminants from Wastewater through Bio-Nanotechnology, 573–604. https://doi.org/10.1016/B978-0-323-85583-9.00008-9.
8. Jabbar, K. Q., Barzinjy, A. A., & Hamad, S. M. (2022). Iron oxide nanoparticles: Preparation methods, functions, adsorption and coagulation/flocculation in wastewater treatment. Environmental Nanotechnology, Monitoring & Management, 17, 100661.https://doi.org/10.1016/J.ENMM.2022.100661.
9. Noruozi, A., & Nezamzadeh-Ejhieh, A. (2020). Preparation, characterization, and investigation of the catalytic property of α-Fe2O3-ZnO nanoparticles in the photodegradation and mineralization of methylene blue. Chemical Physics Letters, 752, 137587. https://doi.org/10.1016/J.CPLETT.2020.137587